NASA TN D-1271

31

TECHNICAL NOTE

D-1271

A SIMPLE SOLAR ORIENTATION CONTROL SYSTEM FOR SPACE VEHICLES

By Seymour Salmirs, S. Lawrence Kessler,
and Otis J. Parker

Langley Research Center
Langley Station, Hampton, Va.

NATIONAL AERONAUTICS AND SPACE ADMINISTRATION
WASHINGTON

September 1962

NATIONAL AERONAUTICS AND SPACE ADMINISTRATION

TECHNICAL NOTE D-1271

A SIMPLE SOLAR ORIENTATION CONTROL SYSTEM FOR SPACE VEHICLES

By Seymour Salmirs, S. Lawrence Kessler, and Otis J. Parker

SUMMARY

A control system for solar orientation of space vehicles has been designed and examined on a single-degree-of-freedom air-bearing platform. The response of the system to various initial errors was measured and phase-plane diagrams of the system performance are presented. Methods of applying control torques are considered, and the application of artificial damping through the proper use of control torques is investigated.

The results show that simplicity may be obtained with the use of reaction jets. It was found that the current system, while suitable for vertical probes, would consume excessive fuel for consideration in satellite vehicles. Calculations based on improvements in the system that are thought to be reasonably achievable indicate that a cold-gas control system may be attractive for certain solar-power-collecting missions. It appears possible to construct a system requiring 2.57 pounds of fuel per axis to control a satellite having inertia of 100 slug-ft^2 to an accuracy of 0.5° for 1 year.

The system tested was found to be capable of pointing accuracies of ± 18 seconds of arc. Possible improvements could increase the accuracy to 0.1 second of arc, without regard to fuel consumption. However, even with extreme improvements in system performance, it is shown that fuel requirements with a cold-gas system render the system impractical for orbital use at these accuracies.

A stable air-bearing design was evolved which successfully simulated the friction-free space environment.

INTRODUCTION

Satellites or vehicles operating in interplanetary space will, in many instances, require accurate information concerning the sun's direction from the vehicle. In some cases, orientation of the vehicle toward

the sun is necessary and desirable. References 1 and 2 describe some of these requirements and methods of achieving them. For example, solar orientation can be used for the following purposes:

(1) Thermal balance

(2) Collection and utilization of the radiated energy from the sun

(3) Interplanetary navigation reference point

(4) Investigation of solar properties

(5) A reference for astronomical telescopic observations

This investigation deals with some preliminary experimental results obtained with a mockup of a single-degree-of-freedom solar orientation control system. The system was mounted on an air bearing to simulate the friction-free space environment. Emphasis was placed on simplicity in the effort to obtain long-term reliability. Methods of applying control torques were considered and the application of artificial damping by the proper use of control torques was investigated. The use of a simple gas-reaction jet-control system in the space environment was considered. The response of the system to various initial errors in the range of 0.5° to 90° was recorded and system time delays were measured.

DESIGN CRITERIA

The most important single consideration in any space vehicle operation is its reliability. Other aspects of the control system design must necessarily be subjugated to this primary factor if long-time operation is intended. As a consequence, less emphasis has been placed on such important problems as weight and power consumption than might have been the case had the maintenance of the equipment in space been a simple matter. Since the essence of reliability is simplicity, it is possible to achieve low weight and low power consumption by holding the system to a very few parts.

The simplest and most common method of obtaining control torques is by the use of reaction jets. A cold gas, hot gas, or vaporizing liquid are all feasible; simple switching circuits may be used, and no proportional amplifiers are required; however, the gas system is definitely limited for long-period operation since all fuel must be carried along.

The same control components may be used to apply current to coils (utilizing the earth's magnetic field) instead of operating a jet valve.

In this case a system with no moving parts may be envisioned. However, relatively complex electronics are required for proper coil activation, since the magnetic field is variable in both strength and direction.

CONTROL-SYSTEM DESCRIPTION

The system investigated consisted basically of a solar sensor, control circuits, and a pair of gas jets. All components including the electrical and pneumatic energy supplies were mounted on a single-degree-of-freedom air-bearing supported platform. A carbon arc lamp was used to simulate the sun. Figure 1(a) is a schematic diagram of the test setup showing the angle-measurement system employed. A mirror was mounted at the center of rotation of the platform to reflect a light spot from a projector onto a moving paper recorder. Figure 1(b) is a photograph of the platform and arc lamp.

Sensor

The sensor used in all the tests consisted of a pair of series-connected silicon solar cells mounted with an acute angle between them. An opaque shield extended from the point of the acute angle between the cells. The function of the shield was to shadow one of the cells and increase the difference in output between the cells. A more complete description of the sensor and its operation may be found in reference 1. An earlier model of the test sensor can be seen in figure 1(b) and a photograph of the sensor calibration device is shown in figure 2. The sensor is seen to include cells mounted on the opaque shield. These cells operated in the same manner as those on the base pyramid and provided a signal from which the rate-limiting system was operated. Sensor calibration curves of output voltage as a function of the error angle θ are presented in figures 2(b), (c), and (d).

Attitude Control

The attitude information was prepared for use by the system by a balanced direct coupled amplifier whose operating characteristics are shown in figure 3. The amplifier became saturated at attitude errors corresponding to 15 seconds of arc. Because of this low-angle saturation, the amplifier was used effectively as a switch, and operated almost entirely in the saturated state. Thus, extremely large amounts of amplifier output drift could be tolerated so long as the system accuracy required is 15 seconds of arc or larger.

Damping

Damping was obtained in three independent ways as shown in figure 4. The first (fig. 4(a)) was the use of a simple capacitor-resistor lead network on the output of the attitude amplifier. This method was extremely limited at very low frequencies because of the very large capacitance required to produce effective time constants. The use of large capacitors brought with it the problems of large volume, weight, and leakage at constant voltages. A second method used (fig. 4(b)) was to amplify the attitude signal and provide a lead around the attitude amplifier. The operation is indicated in the following sketch:

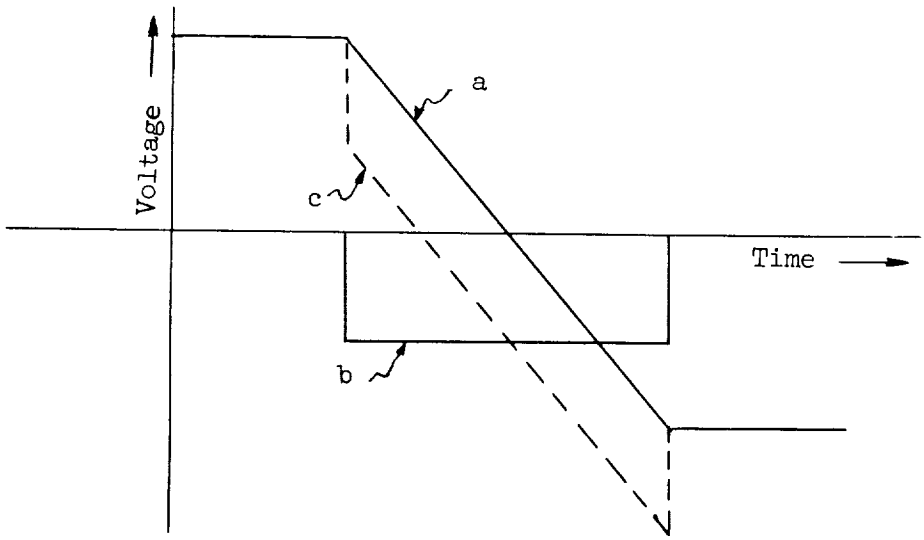

A transformer was used to differentiate the attitude signal a. The differentiated signal b was then added to the original signal, so that the curve c resulted. This curve leads the original signal a. Both the first and second systems were effective only at small error angles because of the sensor-output saturation characteristics.

The third method used (fig. 4(c)) was merely to limit the angular velocity of the vehicle. This result was accomplished by differentiating the signal produced by the cells on the opaque shield. This signal was then combined with the attitude signal. When the rate of change of voltage reached a sufficient magnitude, the torque device was turned off and the vehicle drifted through zero until torque was applied in the opposite direction. Because of the steepening slope of the rate sensor signal shown in figure 2(d), the rate limiting became more effective as zero was approached.

Combination of Attitude and Rate Limiting

An attitude-rate mixer circuit turned the jet valve on in the presence of an attitude error and turned the valve off with the introduction of a rate in the proper direction. The circuit, a block diagram of which is shown in figure 5, may be considered to consist of three sections: (1) the attitude switch, (2) the rate switch, and (3) the valve switch.

The output of the attitude amplifier is applied to the attitude switch, which senses its polarity and provides a signal to the valve switch to actuate the proper solenoid. The output of the rate cells is capacitively differentiated by the use of a simple resistance-capacitance network, with the rate amplifier impedance as the resistive component. After amplification the signal is applied to the rate switch. When this signal is of sufficient magnitude, a second signal is applied to the valve switch to overcome the effect of the attitude signal and deactivate the solenoid.

EQUIPMENT AND TEST PROCEDURE

Air Bearing

Experiments were conducted on a platform mounted on an externally pressurized spherical air-lubricated bearing. This bearing, whose mating surfaces are completely separated by a film of air, provides zero static friction and extremely low friction values during motion. The moving friction is directly dependent upon the shear in the thin air film. However, at the rotational rates considered, essentially no friction was present.

Two types of spherical air bearings were developed and tested. The first type, which uses a single orifice (fig. 6), is externally pressurized through the single orifice in the center. It was designed so that the top of the cavity would be at the maximum diameter of the sphere in order to keep the air escape clearance to a minimum. Tests indicated that this position of the cavity was undesirable because it decreased the resistance to side loads (radial stiffness). Subsequent tests indicated that an angle between the horizontal center line of the sphere and a line passing through the center of the sphere and the top peripheral edge of the cavity of 15° would increase the radial stiffness without appreciable effect on the load-carrying capacity. It was found that this type of bearing has a self-induced vibration due to a poppet action of the sphere as the air escapes. The poppet action, however, was found to be negligible under small loads and very low airflows. Bearings of this type appear to be practical where static conditions and high radial stiffness are not demanded.

The second type of air bearing studied, the multiple-orifice type (fig. 7), is externally pressurized from a radial chamber through two concentric rows of orifices. Tests were made on 2.0-inch- and 4.0-inch-diameter bearings using different arrangements of 0.010-inch- and 0.0135-inch-diameter orifices. An additional exhaust hole in the center stabilizes the bearing by reversing the flow of some of the air between the sphere and cavity thus preventing a poppeting action. If the exhaust hole is of proper size, approximately 65 percent of the air used may be exhausted and ducted away. This capacity enhances the possibility of using the bearing in a vacuum chamber. This bearing has very good load-carrying capacity and radial stiffness. It can operate satisfactorily even under the influence of radial shock loads, a condition that could not exist for the single-orifice bearing. A check on the operation of the bearing was necessary before and after a test run of the control system. The check was accomplished by measuring the electrical resistance between the sphere and cavity.

Early in the program, after what appeared to be exceptionally well-damped tests using a single-orifice bearing, the bearing was found to be making partial contact in that resistance dropped from infinity to several megohms. Friction levels under these conditions were difficult to detect but were certainly under the 0.025 ounce-inch of torque supplied by the jets in these tests. This increased friction level was sufficient to produce excellent results and is indicative of the damping required and the simulation effort required.

Figure 8 shows the difference in the curves of maximum load-carrying capacity as a function of supply air pressure for the single-orifice and the multiple-orifice bearings of 2-inch diameter. The curve for the theoretical maximum load-carrying capacity as a function of air supply pressure for a multiple-orifice bearing was empirically derived and was found to be based on the product of the air pressure and 68 percent of the effective projected area.

Figure 9 shows the difference between the flow of air required as a function of maximum load-carrying capacity with the two types of bearings.

Figure 10 shows the oscillation of the table with no torques applied other than the spring constant of a wire to the center of rotation of the table from the ceiling. This wire was used on occasion to record various quantities during operation. It consisted of shielded four-conductor thermocouple leads made of strands of No. 30 braided copper wire.

Energy Supply

It was necessary to include all the energy required by the control system on the test platform since the torque introduced to the platform from even a single wire was sufficient to affect the test results. Standard aircraft large-capacity storage batteries and smaller dry cells were used to supply all electrical power. The size of the batteries seen in figure 1(b) was governed by the desire to run many series of tests without having to recharge often rather than by the actual requirements of the system. Since only a single degree of freedom was being considered in these tests and balance was a small problem, it was not necessary to use hermetically sealed batteries.

The gas supply was contained in a high-pressure bottle. The gas used was nitrogen at 1,500 pounds per square inch and was selected only on the basis of availability. The gas system used in these tests provided a torque T of 0.036 foot-pound. The platform inertia I was approximately 24.5 slug-foot^2.

Data Recording

The data taken in these tests consisted of recordings of the response of the system to various initial errors and were obtained optically. A light was projected onto a mirror mounted on the center of rotation of the platform and reflected onto a moving paper at distances of 30, 105, and 201 inches from the mirror. The spot of light was traced with a pencil to produce the recording. The paper had graduations of 0.14 inch, representing platform deflections of approximately 8.0, 2.3, and 1.2 minutes of arc, respectively, at those distances. With the manual recording system being used, the resolution of the recording was believed to be approximately one-half division of about ±2 minutes of arc, ±35 seconds of arc, and ±18 seconds of arc, for distances of 30, 105, and 201 inches, respectively.

It was found necessary to restrict the movements of people in the room while tests were being conducted. Normal walking at distances of 10 feet away caused air currents, so that platform motions of as much as 2 minutes of arc were produced. Building vibrations, such as closing doors at some distance away caused similar difficulties.

Four tests were made after each alteration to the platform control system. The platform was held at initial errors of approximately 0.5°, 1.5°, 25°, and 90° and released, and the response noted. In each case the platform was released manually, an attempt being made to hold the platform as steady as possible prior to release. Considerable practice permitted the operator to release the platform at the desired angle and almost zero angular velocity. The zero time point on the data was taken

as the point at which zero angular velocity occurred. The four initial error settings were selected from the sensor calibration curves of figures 2(b) and (c). The 0.5° error is on a portion of the curve with a very high slope, the 1.5° error is on that part of the curve where the slope is reducing, and the 25° and 90° errors are on that part of the curve where the slope is very small. For large initial angular errors, a rate gyro was added to the platform to provide information on the rate switching circuits.

System Time Delay

The overall system time delay was measured by installing a crude hot-wire anemometer in the jet nozzle. A switch supplied a step input to the system and simultaneously actuated an oscilloscope trace. The change of current through the hot wire caused the trace to deflect vertically. The trace was photographed and the time delay was measured from the trace. A schematic diagram of the arrangement is shown in figure 11(a), and a sample oscilloscope trace is shown in figure 11(b). A time delay of about 10 milliseconds was measured. The hot wire used was a straight filament of a very small light bulb with a low voltage supplied to the bulb. The filament was inserted in the nozzle, and the voltage on the filament was varied to provide proper sensitivity for the airflow measurements and to avoid saturation.

RESULTS AND TESTS

Attitude Signal Only

The configuration providing attitude signal only consisted simply of the jet with sensor and amplifier feedback. The system oscillated and showed no marked tendency to change amplitude in approximately 8 minutes of operation. A portion of this oscillation is shown in figure 12. It may be inferred from this figure that air damping was present and was of sufficient magnitude to overcome the system lag. The only feature of this arrangement was to show the level of air damping and the degree of success in simulating the space environment. In space the system lag would have been sufficient to cause divergence.

Jet Reaction With Capacitor Lead

The jet-reaction system with the capacitor lead was able to damp to ± 2 minutes of arc in about 6 minutes from an error angle of -3°, as shown in figure 13. The lead achieved was quite small and insufficient by itself, even with a capacitor of 3,000 microfarads with a time constant of 0.3 second.

Jet Reaction With Transformer Lead

The jet reaction with the transformer lead was adequate at small angles. The system was observed to damp from an initial error of 1° to a final angle of about ± 18 seconds of arc (the limit of resolution of the measuring system) in about 130 seconds. However, from large angles, the damping supplied in this manner was entirely insufficient, requiring inordinately large times to damp. It should be noted that with the use of a proportional system, this type of damping may prove more profitable.

Rate Limiting

The rate-limiting system (fig. 14) appeared to be the most satisfactory for use in capturing the light source from large angles. The system was observed to damp from 90° to a limit cycle of ± 4.1 minutes of arc in 180 seconds, with the oscillation reducing to one-half amplitude in less than one cycle. The rate resolution of the system was 0.115° per second, as determined by the rate gyro mounted on the platform. Figure 14 shows the time history and a phase-plane diagram of the system operation from an error angle of 67°. The recording system was incapable of recording angles higher than this value; consequently, no data are presented beyond 67°.

In the following discussion a number of terms are used which are now defined for clarity. The first of these items is the "rate resolution." This term refers to the lowest angular rate at which the jet valves are cut off and is the lowest level of rate limiting. Secondly, the "attitude resolution" is the smallest attitude error angle at which the valves are turned on. Third, the "system resolution" is the maximum pointing error of the system in its final limit cycle. The gains referred to in the succeeding paragraphs are multiples of improvement in the experimental resolutions, that is, a gain of 100 in rate refers to a rate resolution 100 times lower than the experimental value.

The phase planes are represented as plots of the nondimensional attitude angle Ω as a function of nondimensional angular velocity $\dot{\Omega}$. The unique method of obtaining dimensionless parameters for attitude and rate and thereby being able to read values of time easily from the phase plane is presented and analyzed in reference 3. This method is included herein because of the importance of the times in the limit cycle and the ease with which these times may be obtained. Along the constant thrust path on the phase-plane plot, the time in seconds

$$\Delta t = \Delta\dot{\Omega}$$

and along the constant velocity path

$$\Delta t = \frac{\Delta\Omega}{\dot{\Omega}(0)}$$

where

Ω nondimensional angular error (error angle divided by the angular acceleration and unit time squared)

$\dot{\Omega}$ nondimensional angular velocity (angular velocity divided by the angular acceleration and unit time)

$\Delta\Omega$ difference between two points on the constant velocity path

$\dot{\Omega}(0)$ angular velocity at which $\Delta\Omega$ is measured

$\Delta\dot{\Omega}$ difference between points on the constant thrust path

APPLICATION OF RESULTS

The energy of the sun may be utilized by direct conversion into electrical energy through the use of silicon cell arrangements. Parabolic collectors may also be used to collect and concentrate solar energy to achieve temperatures sufficient to operate a heat-cycle engine, to operate thermionic conversion units, or to operate silicon cells at a higher light flux level. The pointing requirements for the simple solar panel arrangement that will produce 95 percent of the attainable power are errors up to about $\pm 18^\circ$. A heat engine would require parabola pointing accuracies of about $\pm 0.5^\circ$; thermionic units may require pointing accuracies of about $\pm 0.1^\circ$ for the same efficiencies. If silicon solar cells are used in combination with a parabolic collector, less critical pointing accuracies than that required for a heat engine may be required.

Limit Cycle

The pointing requirement of the heat engine, or concentrated silicon cells, was examined for the control-system functions needed. Figure 15(a) shows a nondimensional phase-plane plot of a modification of the experimental rate-limiting system. The system resolution was extended to ± 30 minutes of arc, the vehicle-controlled inertia was assumed to be 100 slug-feet^2, and the assumed control torque was 0.04 foot-pound. The rate resolution is that of the present system, 0.115° per second. Achievement of these conditions requires that the

attitude resolution be extended from approximately 0.5 second of arc to 12.7 minutes of arc. The resulting limit cycle has a period of 27.5 seconds and a total valve-on time of 20.1 seconds. The fuel consumption, with cold nitrogen gas considered for this system, would be about 0.38 pound per hour. In 1 year the fuel consumed in the limit cycle alone would be about 3,300 pounds. These figures indicate that while the system may have use (and indeed may be attractive) for a vertical probe, the fuel consumption is such that the present system would be obviously of no value in an orbital vehicle.

Figure 15(b) shows a phase-plane plot of the same system with only the rate resolution modified. A gain of 100 in rate resolution is used, and a resulting limit cycle period of 0.483 hour is obtained. The total valve-on time is reduced to 0.2 second. Each valve would operate approximately 18,000 times in a year, and the fuel consumption for the year would be about 0.47 pound. This value is comparable to the fuel loss that might occur due to valve leakage.

The experimental system has been designed and constructed as an experiment. It may be expected that any system actually used in a vehicle would be an improvement. Several methods of obtaining improvements can be suggested from an examination of the experimental equipment. For example, capacitors having higher capacitance and less leakage are readily obtainable; an increase in the number of silicon cells used for the rate signal would increase the signal slopes; higher gain amplifiers are also available. Since the rate circuit is a derivative system, the noise of the signal source must be considered if the resolution is to be improved. If the silicon cells are assumed to operate in a completely unsaturated manner in response to the received solar energy, calculations show that approximately a 10-percent variation in the solar constant at a frequency of 1 cycle per second would be required to provide a noise level comparable to the signal level at the reduced rate resolution. From these considerations it may be concluded that the improvement in the rate system is not impossible and its attainment indeed seems quite reasonable. Naturally, more effort must be expended before the actual improvement attainable may be determined. For the purpose of this discussion, however, it seems reasonable that a rate gain of 100 may be considered.

Solar Power Mission

If a polar orbit is assumed to provide the vehicle with sight of the sun for its lifetime at a high altitude where the aerodynamic torques are at a minimum, the fuel required would depend on the inertia ratio (which affects the gravitational torques), the center-of-pressure location (which affects the aerodynamic torques), the limit cycle, and disturbing torques (meteorites, magnetic field, internal equipment, etc.).

At an altitude of 900 miles the aerodynamic torque on a 30-foot-diameter collector probably would not exceed 3.0×10^{-6} foot-pound, depending on the configuration of the vehicle. This torque would consume approximately 0.3 pound of nitrogen per year. Gravitational torques, even for a vehicle with a large inertia ratio, would not exceed the aerodynamic torques. Disturbance torques depend almost entirely on the vehicle function and specific design. A supply of 1.0 pound of fuel per year may be included to make allowances for these sources of disturbance. Thus, the total fuel required for a single axis of control is found to be less than 2.57 pounds per year for this particular vehicle and orbit selection. These fuel requirements are summarized in table I.

Astronomical Pointing Reference Mission

The requirements for an astronomical reference are cited as approximately 0.1 second of arc in reference 2. The attitude signal must be extremely high gain and the rate resolution must be of a fine order of magnitude. With the rate resolution of the present system at the best accuracy achieved (±18 seconds of arc), the valves are on almost continuously, although they are turned on at about 0.5 second of arc. Figure 16(a) is a phase-plane plot of the control system for an assumed gain of 10 in attitude and sufficient rate to achieve the pointing accuracy of 0.1 second of arc. The rate gain required is 143 times that available. The valve-on time is 0.14 second per cycle and the period is 0.209 second.

The phase plane of figure 16(b) shows the limit cycle with the rate resolution increased by a factor of 1,000 and an attitude gain of 5; the total valve-on time is 0.02 second, and the period is 0.96 second. The fuel consumed during the limit cycle in 1 hour is 0.11 pound for these conditions. Approximately as much fuel is consumed in 4 hours as would be required for the solar pointing at the larger allowable error of $\pm 0.5^{\circ}$ for 1 year. For an error of 0.1 second of arc, the individual valves are on for only 0.01 second. This time allowance calls for valves of unusually fast response. The valves currently being used had a time constant for thrust buildup of 0.015 second. Because of the valve time constants, it is obvious that some form of lead is required in addition to the rate limiting in order to overcome a practical value of valve time constant. With these improvements, the system could be used for limited times in a vertical probe. The improvements are, of course, orders of magnitude more than can readily be considered feasible. Even if they are assumed to be obtainable, it is obvious that a gas-reaction system will have no use by itself at such fine pointing accuracies in an orbiting vehicle.

CONCLUSIONS

An experimental control system for solar orientation of space vehicles has been designed and examined on a single-degree-of-freedom, air-bearing supported platform. A satisfactory simulation of a friction-free space environment was obtained by using an extremely stable air bearing which was relatively easy to construct. The investigation has led to the following conclusions:

1. The simple orientation system, suitable for use in a space environment, can permit solar orientation in vertical probe experiments, with pointing accuracies of better than 0.5°.

2. Calculations for the experimental system with improved rate gains show that the system using cold nitrogen gas may be suitable for orbital use for periods of about 1 year.

3. Experimental pointing accuracies of about ± 18 seconds of arc were achieved. Calculations show that it may be possible to achieve accuracies of 0.1 second of arc for short periods.

4. Calculations based on extensive system improvements show that continued pointing accuracies of 0.1 second of arc for a space vehicle using a cold-gas system are impractical.

Langley Research Center,
National Aeronautics and Space Administration,
Langley Station, Hampton, Va., April 20, 1962.

REFERENCES

1. Spencer, Paul R.: Study of a Solar Sensor for Use in Space-Vehicle Orientation Control System. NASA TN D-885, 1961.

2. Gillespie, Warren, Jr., Eide, Donald G., and Churgin, Allen B.: Some Notes on Attitude Control of Earth Satellite Vehicles. NASA TN D-40, 1959.

3. Pistiner, Josef S.: On-Off Control System for Attitude Stabilization of a Space Vehicle. ARS Jour., vol. 29, no. 4, Apr. 1959, pp. 283-289.

TABLE I

ONE-YEAR FUEL REQUIREMENTS FOR SOLAR ORIENTATION CONTROL USING COLD NITROGEN FOR ONE AXIS OF CONTROL

[Assumptions: Polar orbit, 900-statute-mile altitude; control-axis inertia, 100 slug-ft^2; 30-foot-diameter collector]

Item	Consumption per axis, lb	
	Rate gain 1.0	Rate gain 100
Limit cycle	3310.0	0.47
Aerodynamic torque	0.3	0.3
Gravitational torque	0.3	0.3
Mechanical disturbances	1.0	1.0
Leakage	0.5	0.5
Total	3312.1	2.57

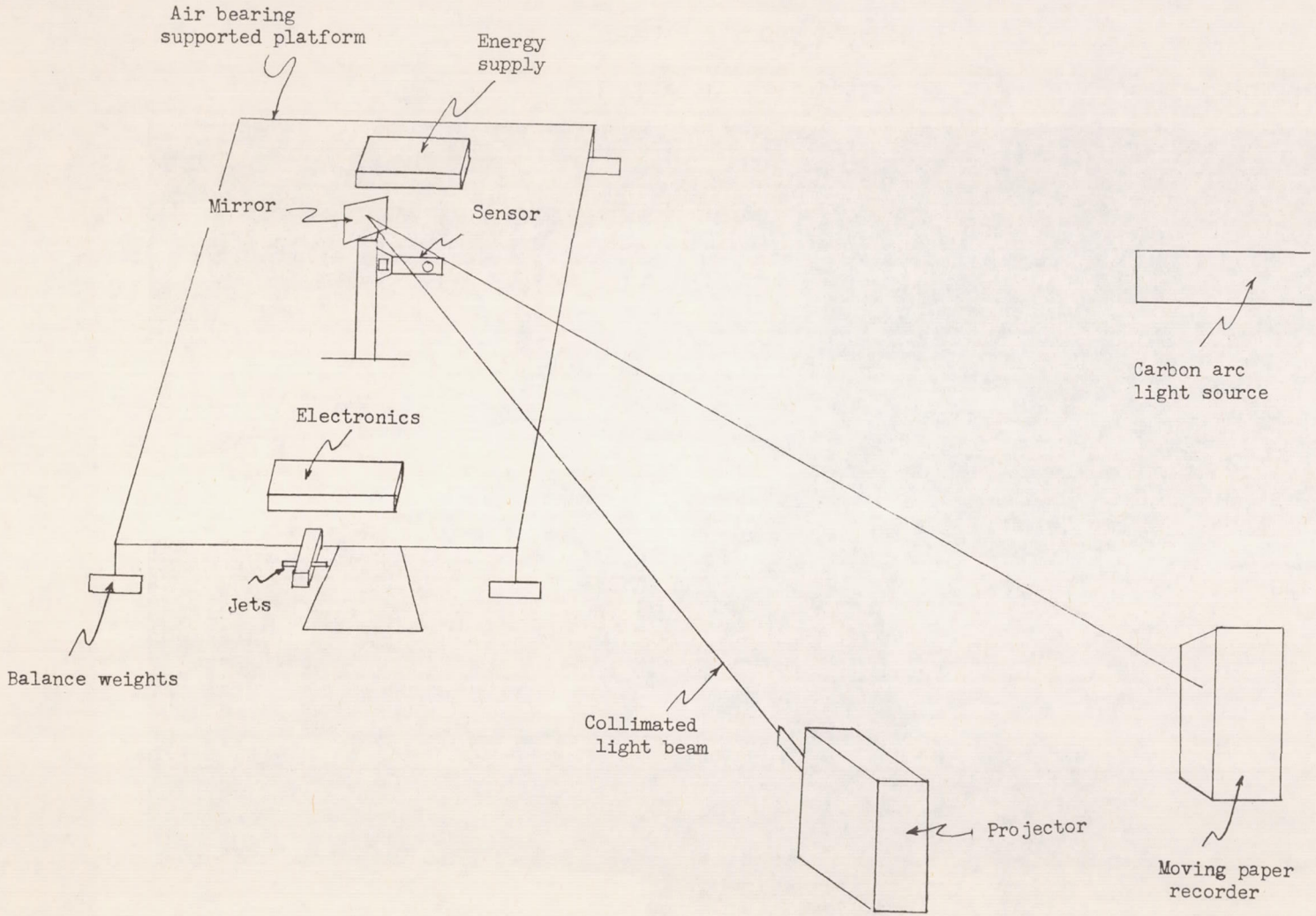

(a) Schematic diagram.

Figure 1.- Control-system test apparatus.

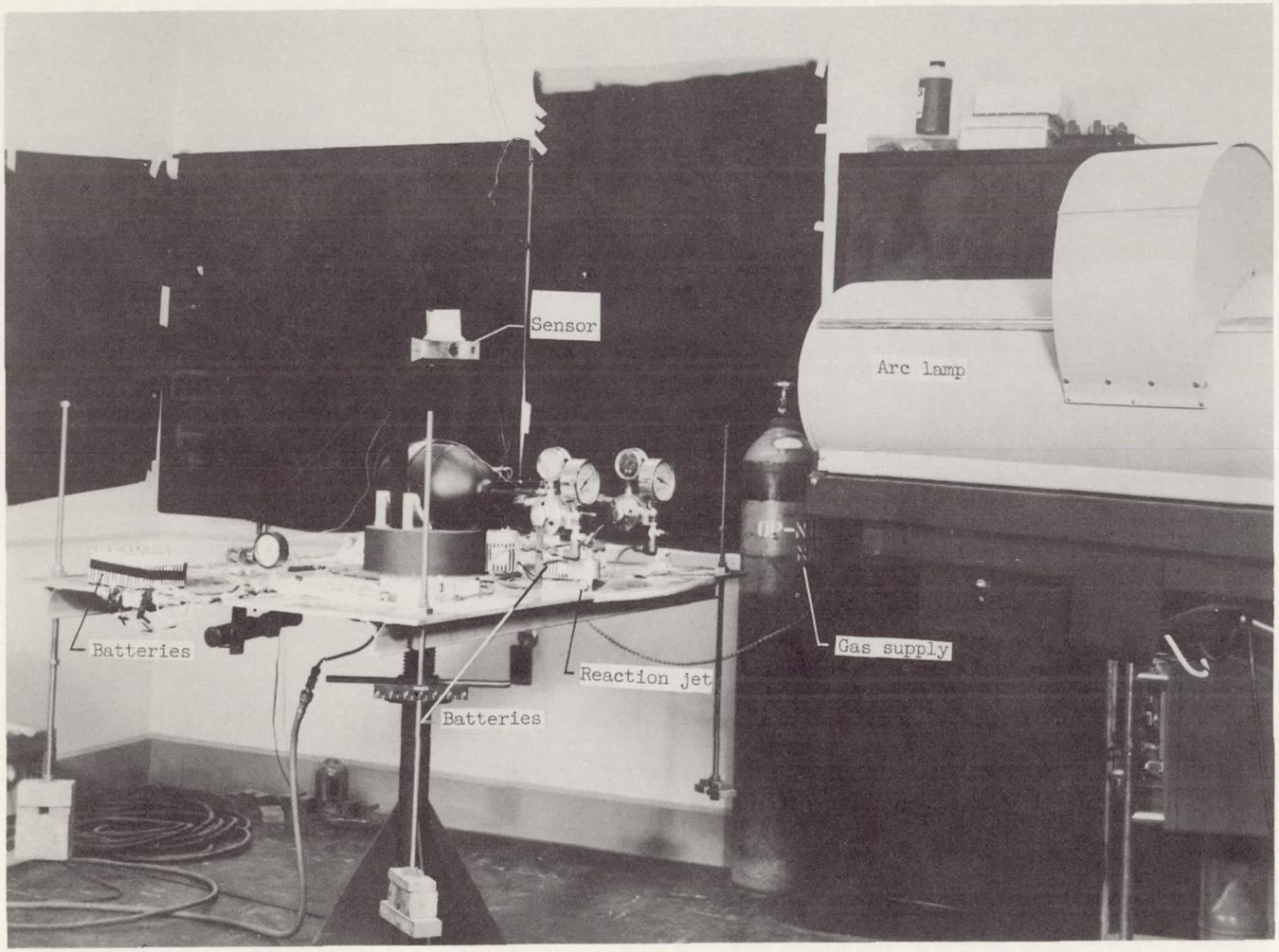

(b) View of test apparatus. L-61-6338.1

Figure 1.- Concluded.

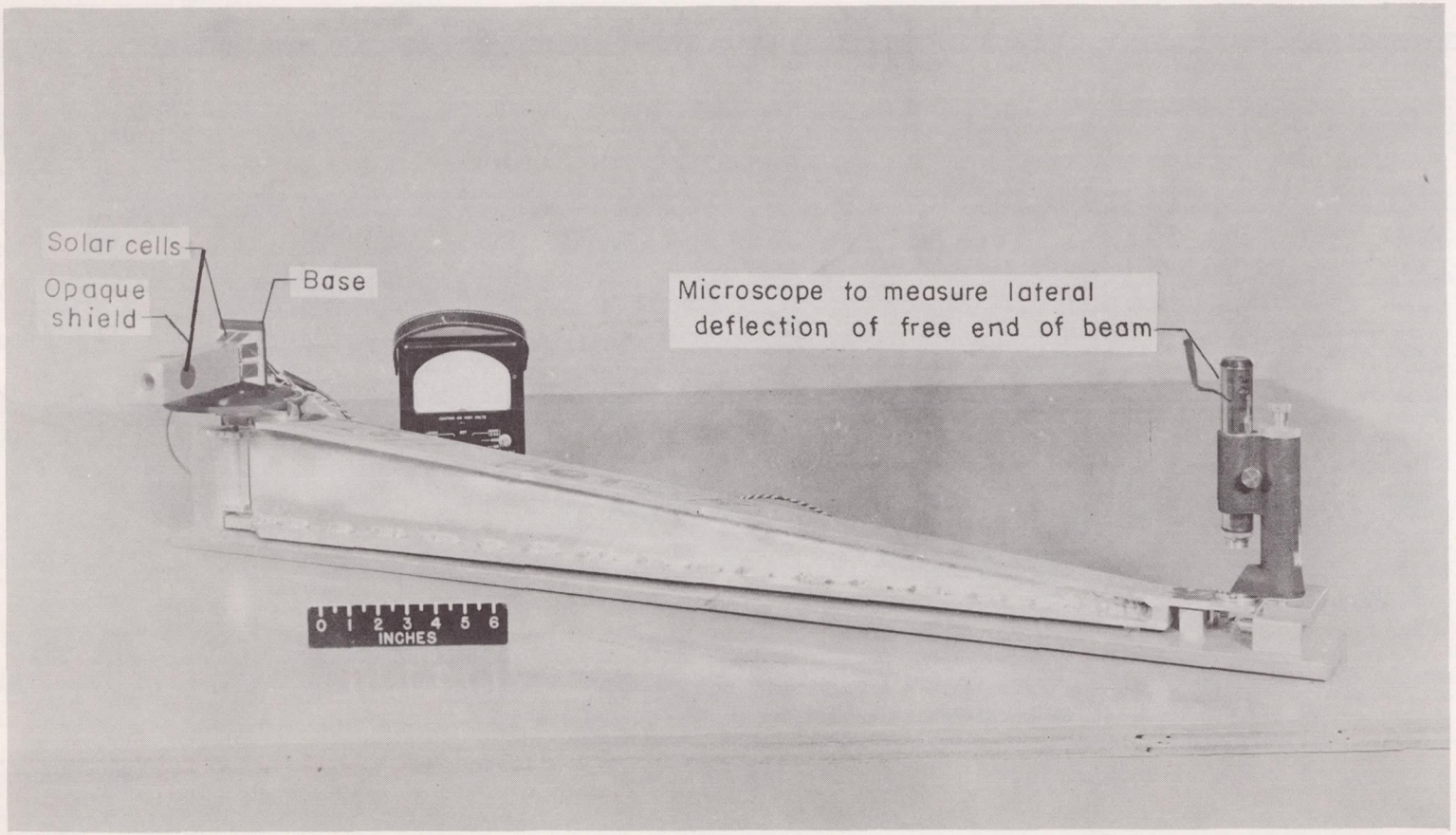

L-60-4664.1

(a) Experimental version of solar sensor attached to I-beam for small-angle calibration. Circular cells in shield provide separate signal to sense angular velocity.

Figure 2.- Solar sensor configuration and calibrations.

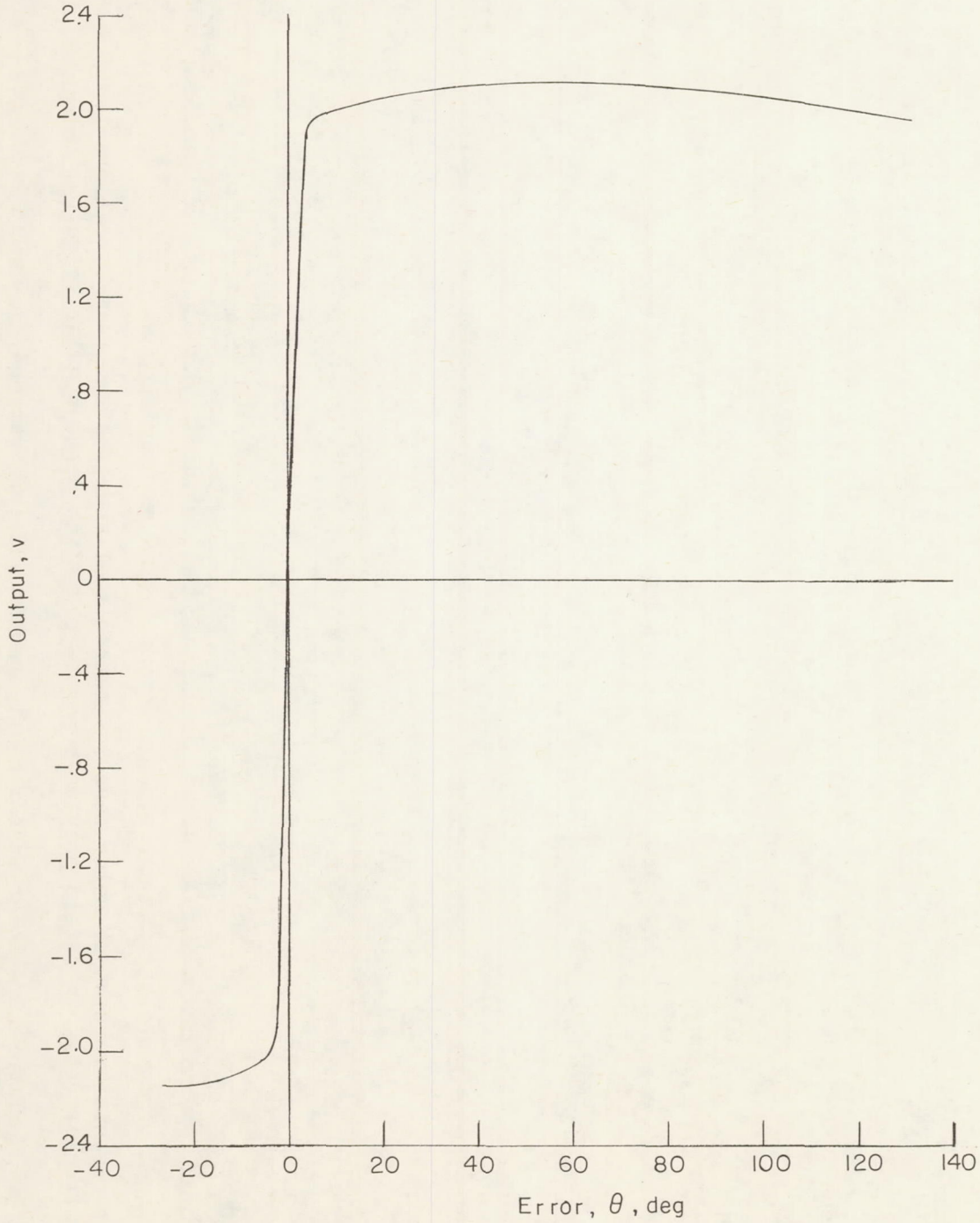

(b) Large-angle calibration.

Figure 2.- Continued.

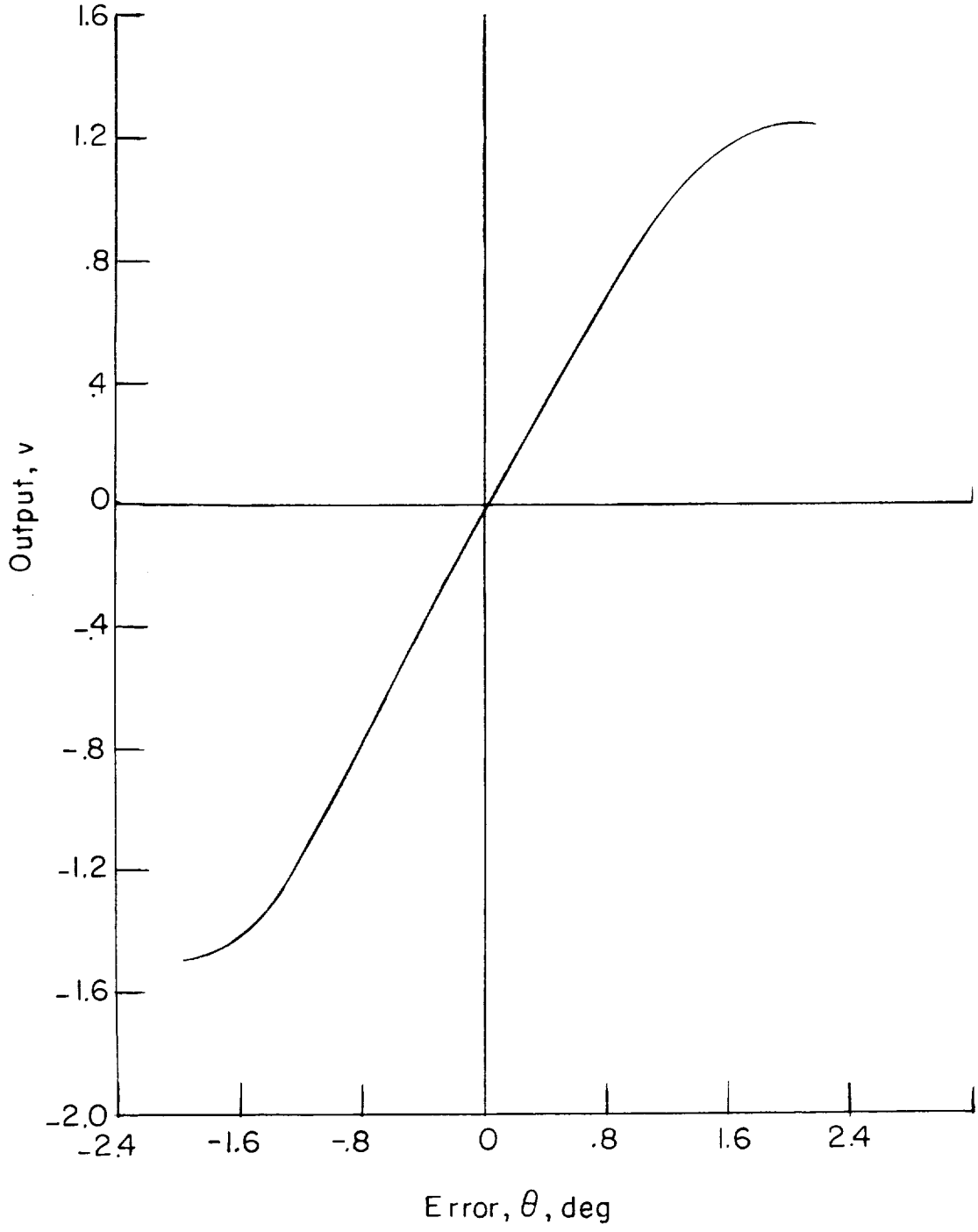

(c) Small-angle calibration.

Figure 2.- Continued.

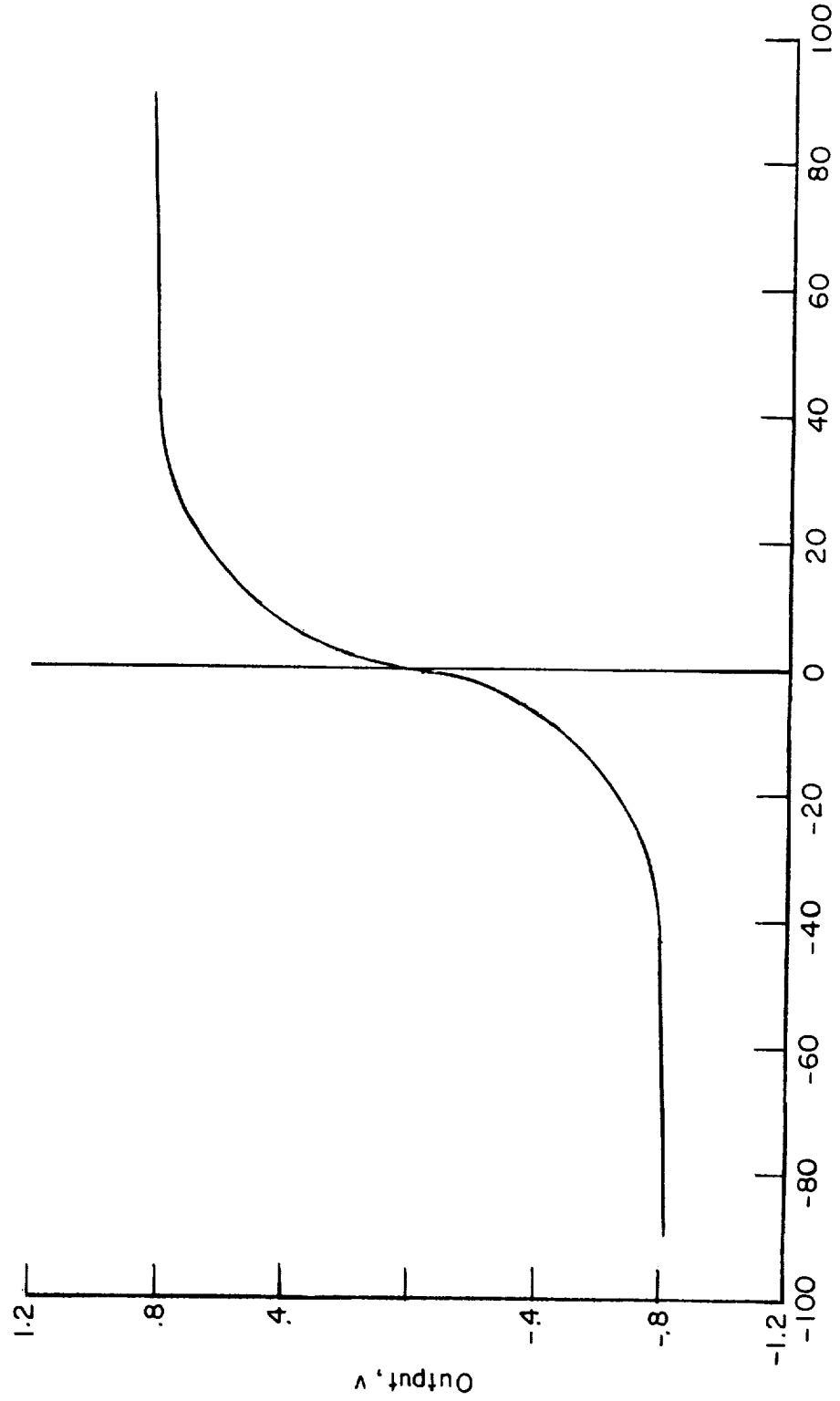

(d) Rate-sensor output.

Figure 2.- Concluded.

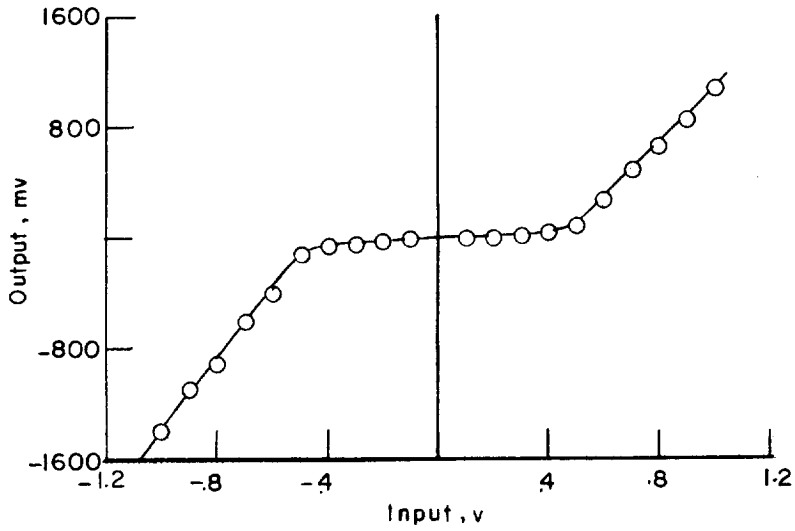

(a) Low level.

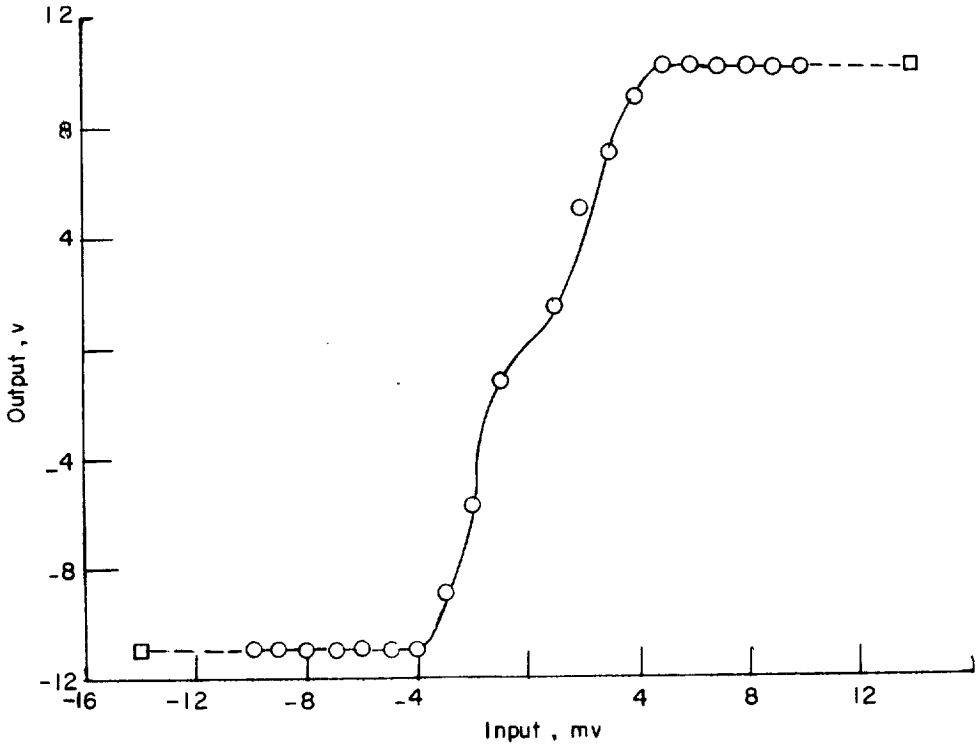

(b) High level.

Figure 3.- Amplifier calibration.

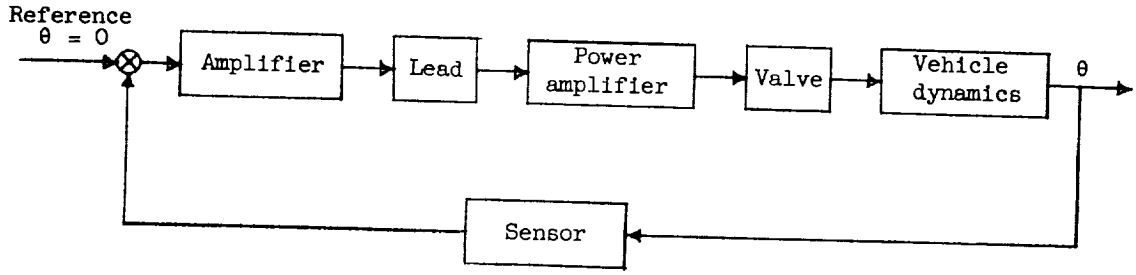

(a) Capacitor resistor lead.

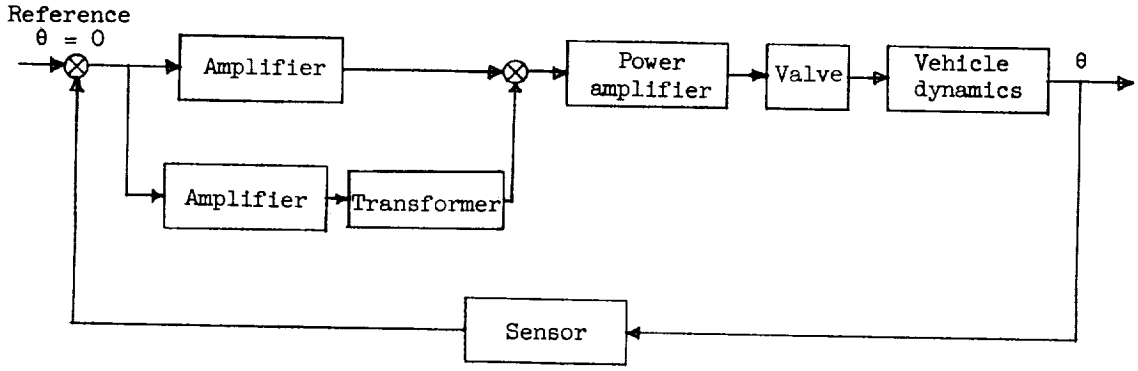

(b) Transformer lead.

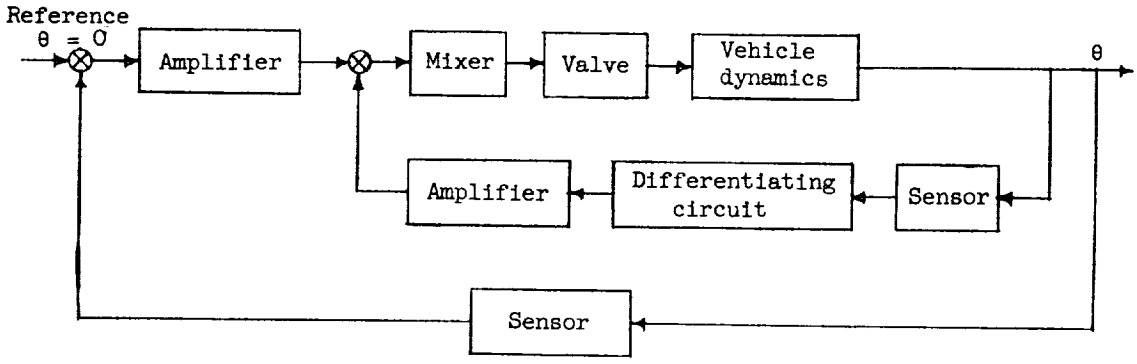

(c) Rate limiting.

Figure 4.- Control-system block diagrams.

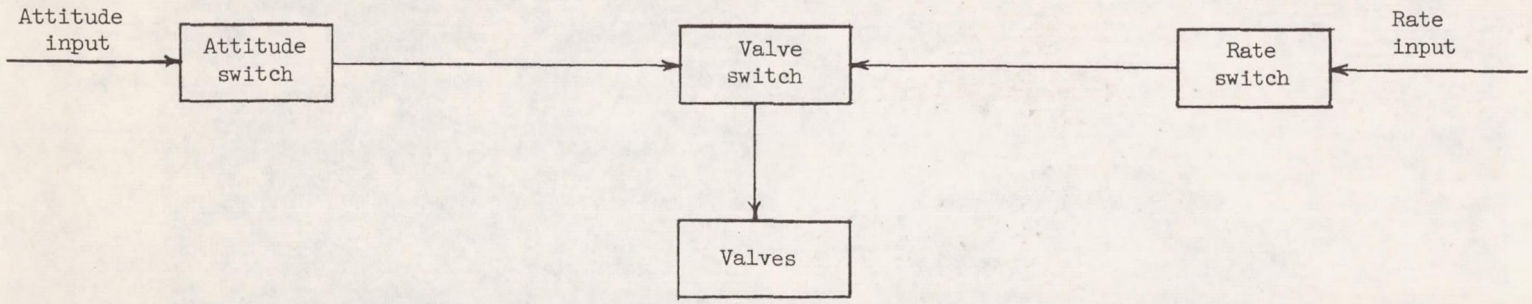

Figure 5.- Attitude-rate mixer.

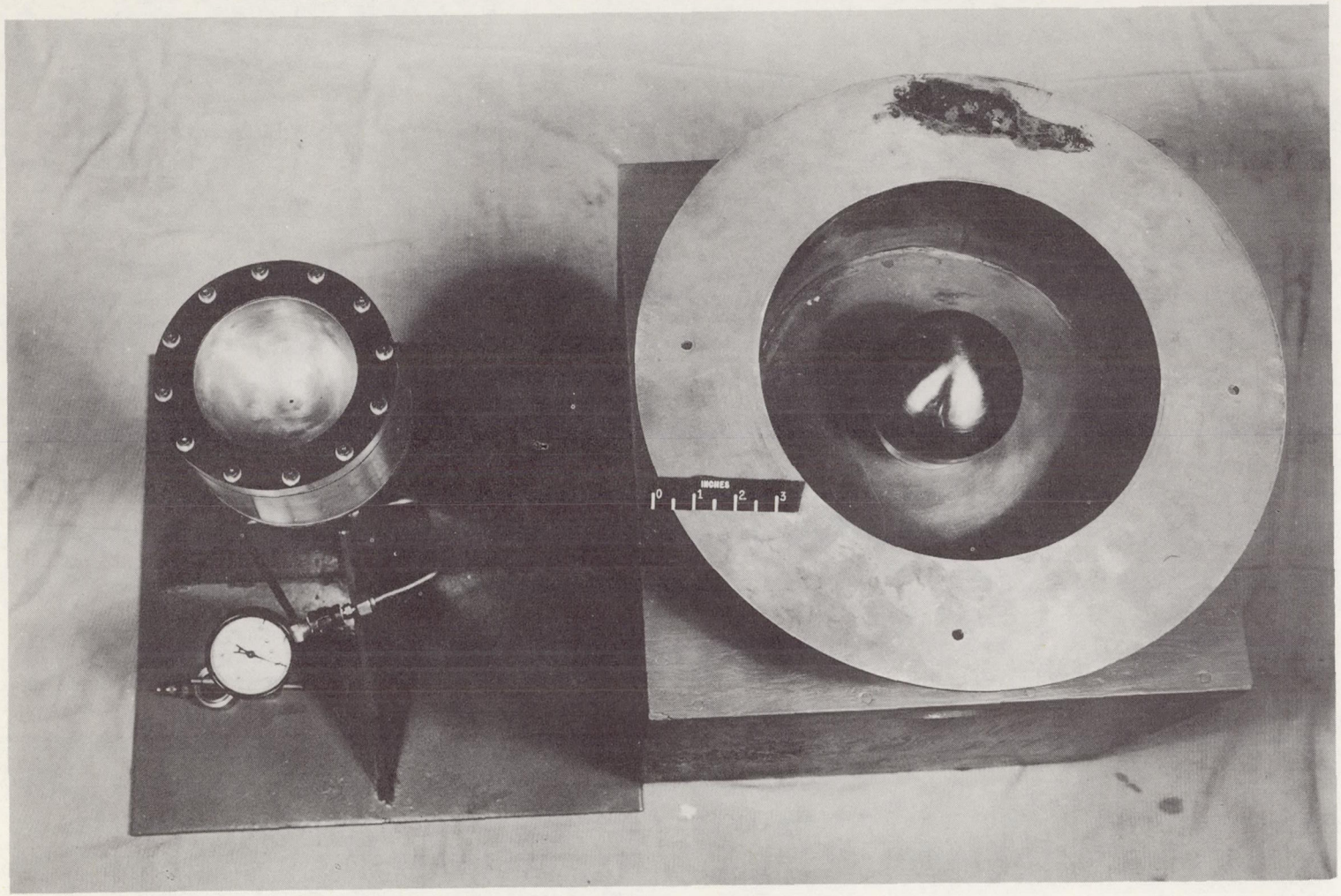

Figure 6.- Single-orifice air bearing. L-59-5365

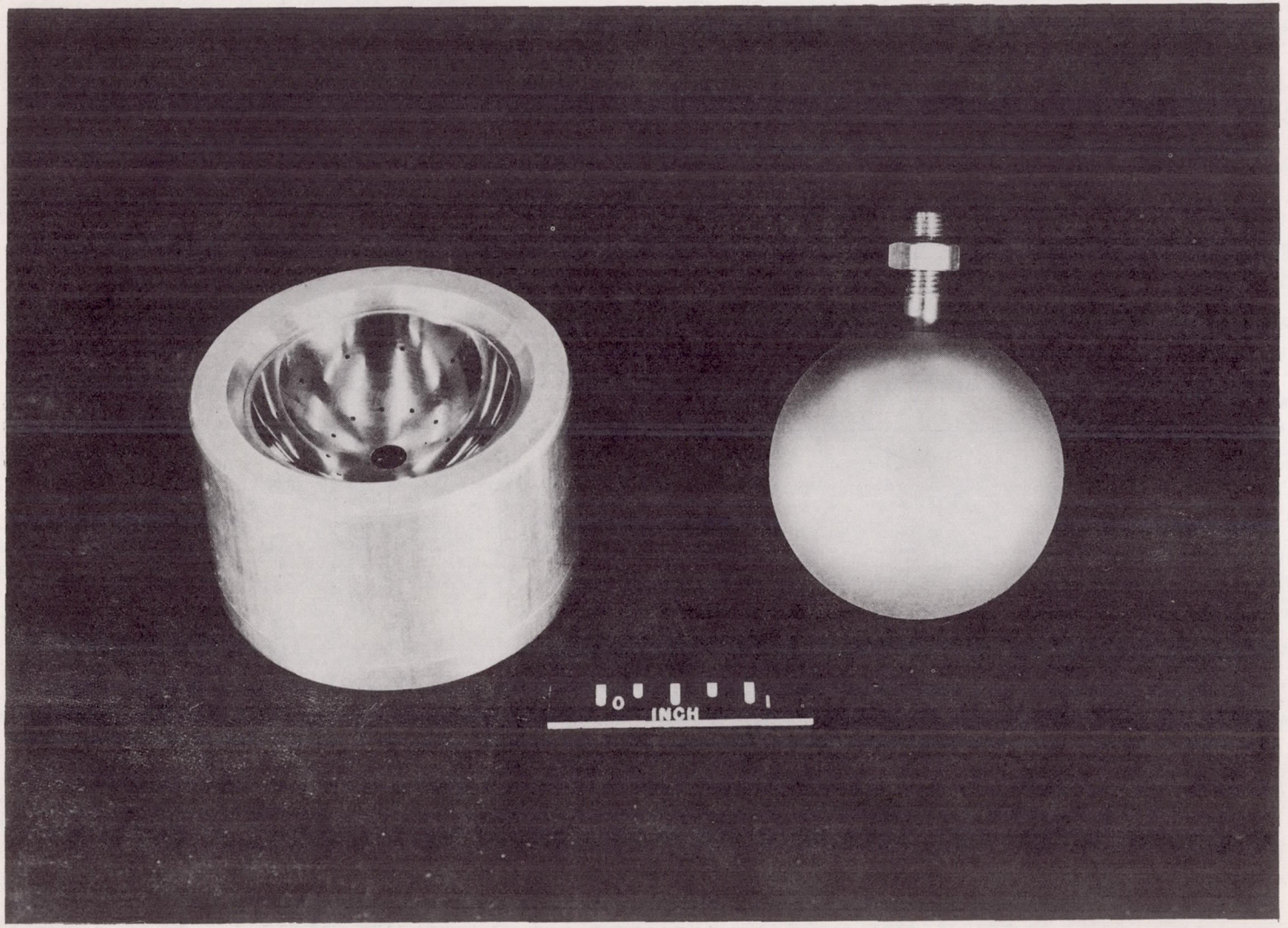

Figure 7.- Multiple-orifice air bearing. L-61-5378

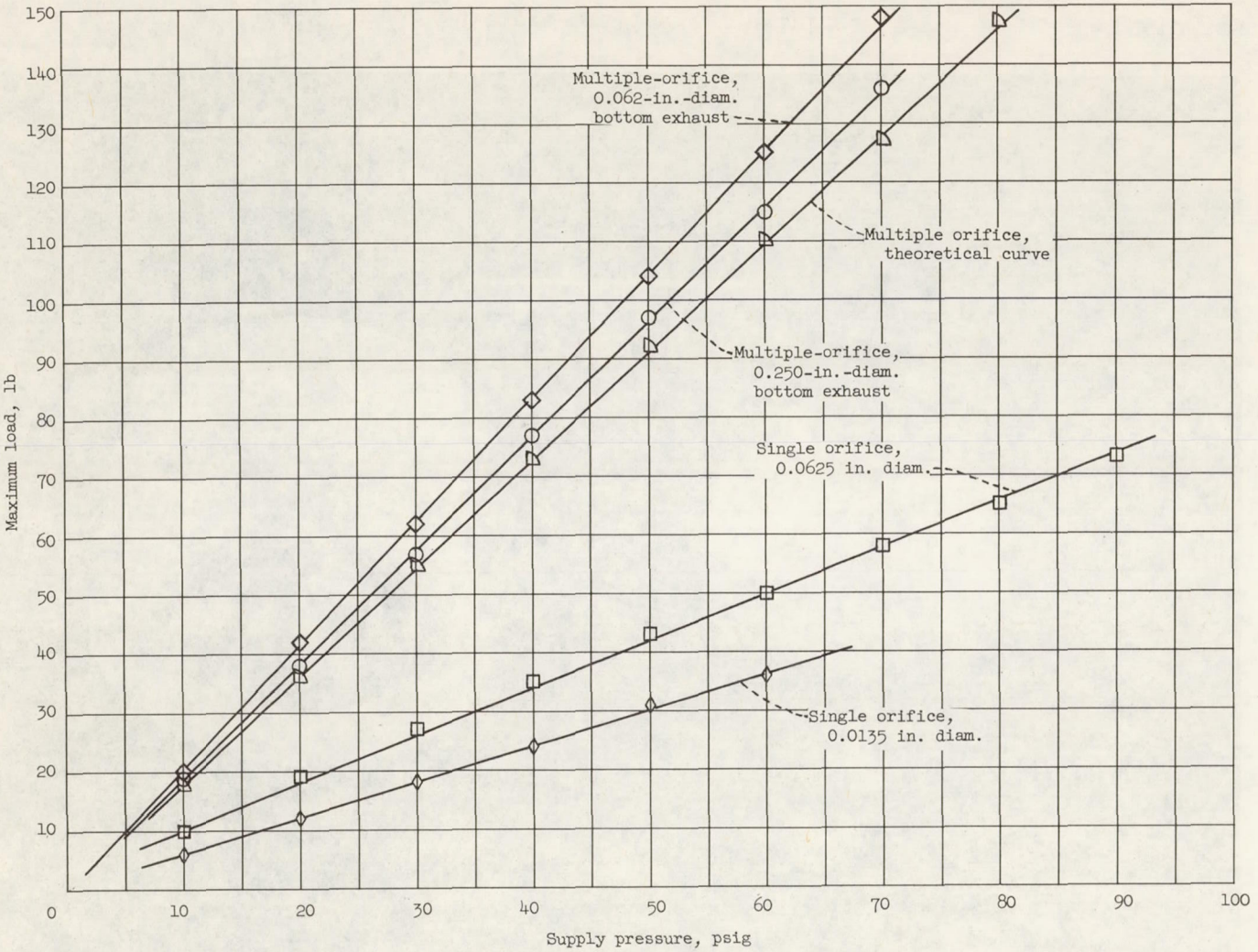

Figure 8.- Maximum load as a function of supply pressure with single-orifice and multiple-orifice air bearings of 2.0-inch diameter.

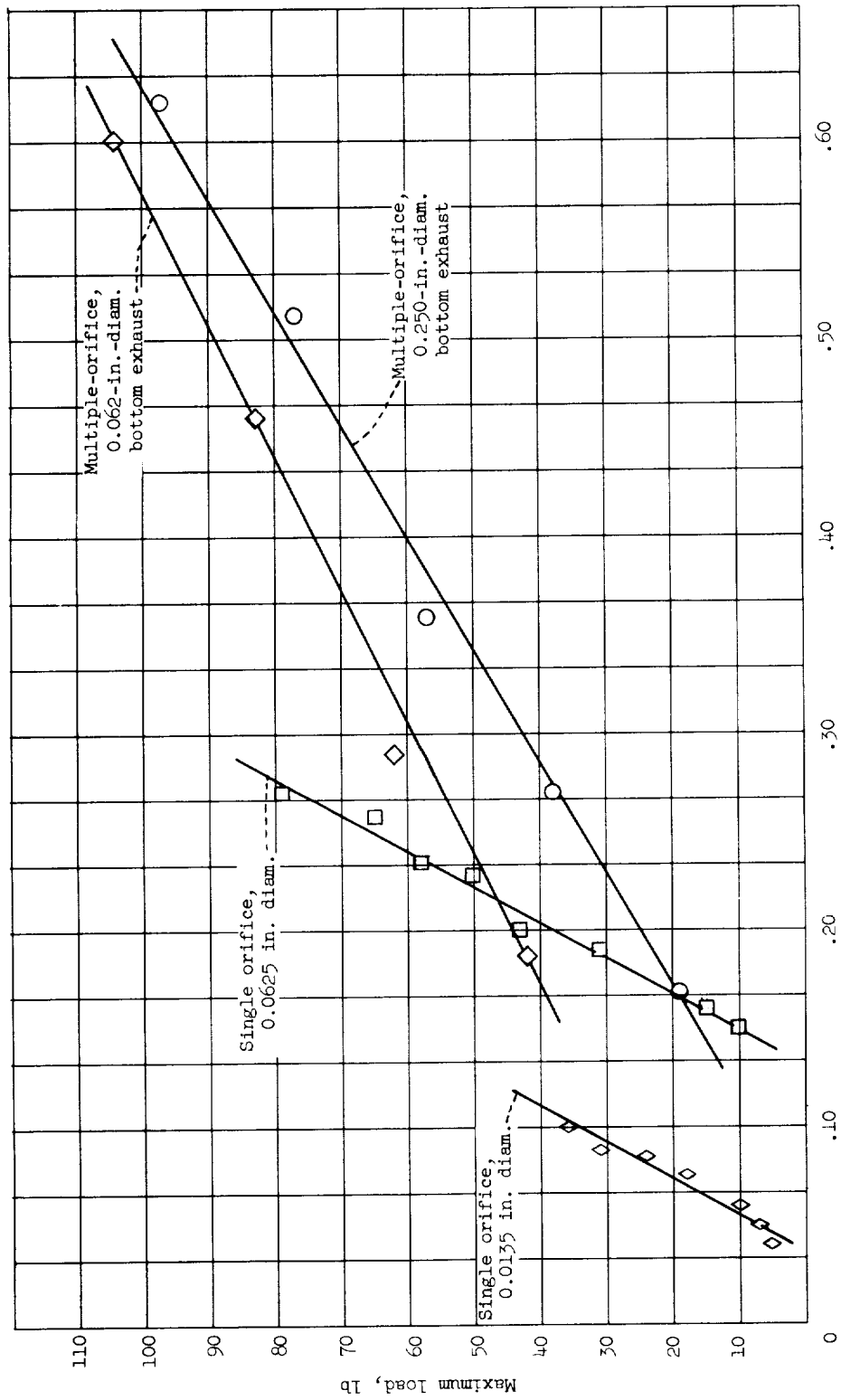

Figure 9.- Maximum load as a function of airflow for single-orifice and multiple-orifice air bearings of 2.0-inch diameter.

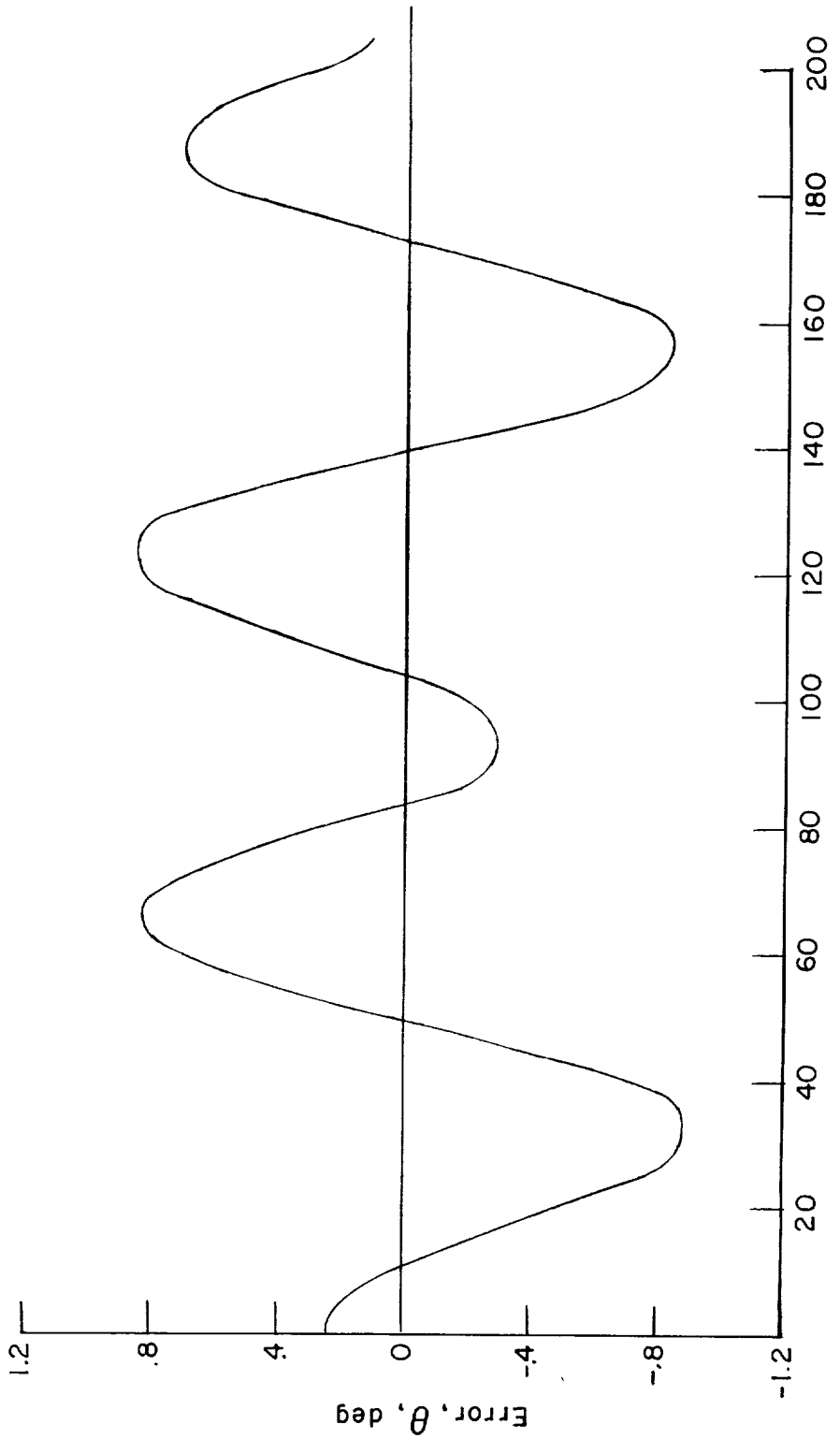

Figure 10.- Platform random motion with instrumentation wires. Controls off.

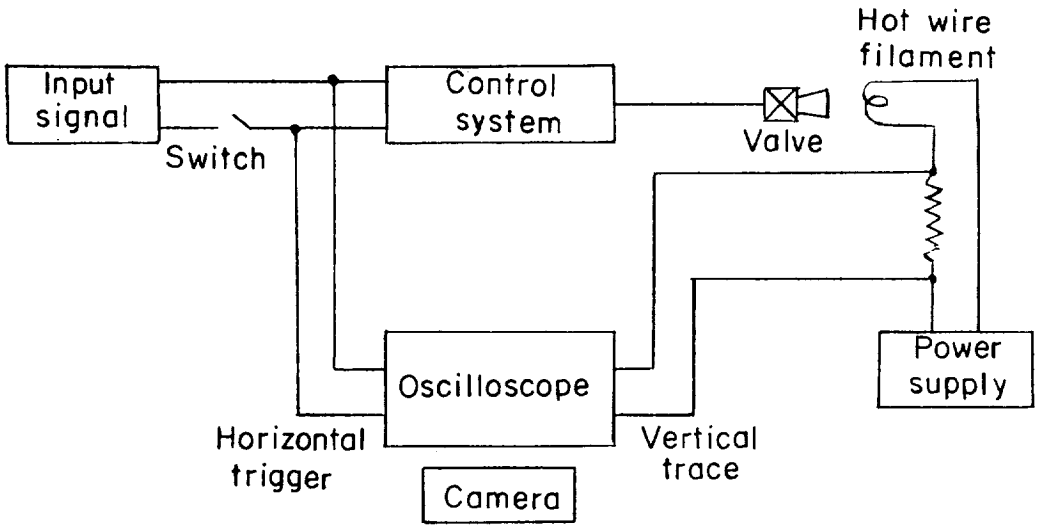

(a) Schematic diagram of measuring equipment.

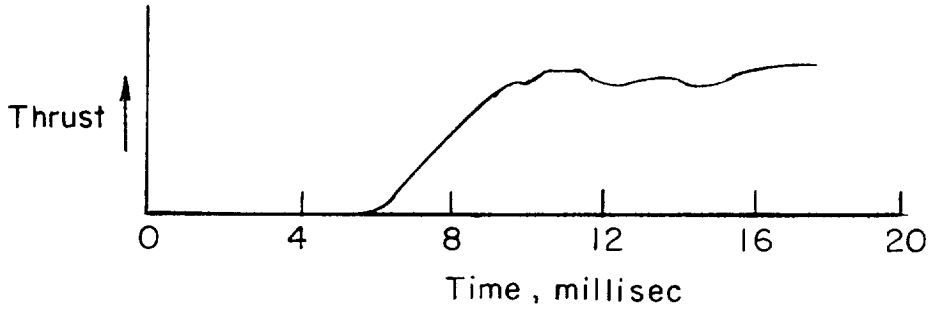

(b) Nozzle thrust recording.

Figure 11.- System time delay measurement.

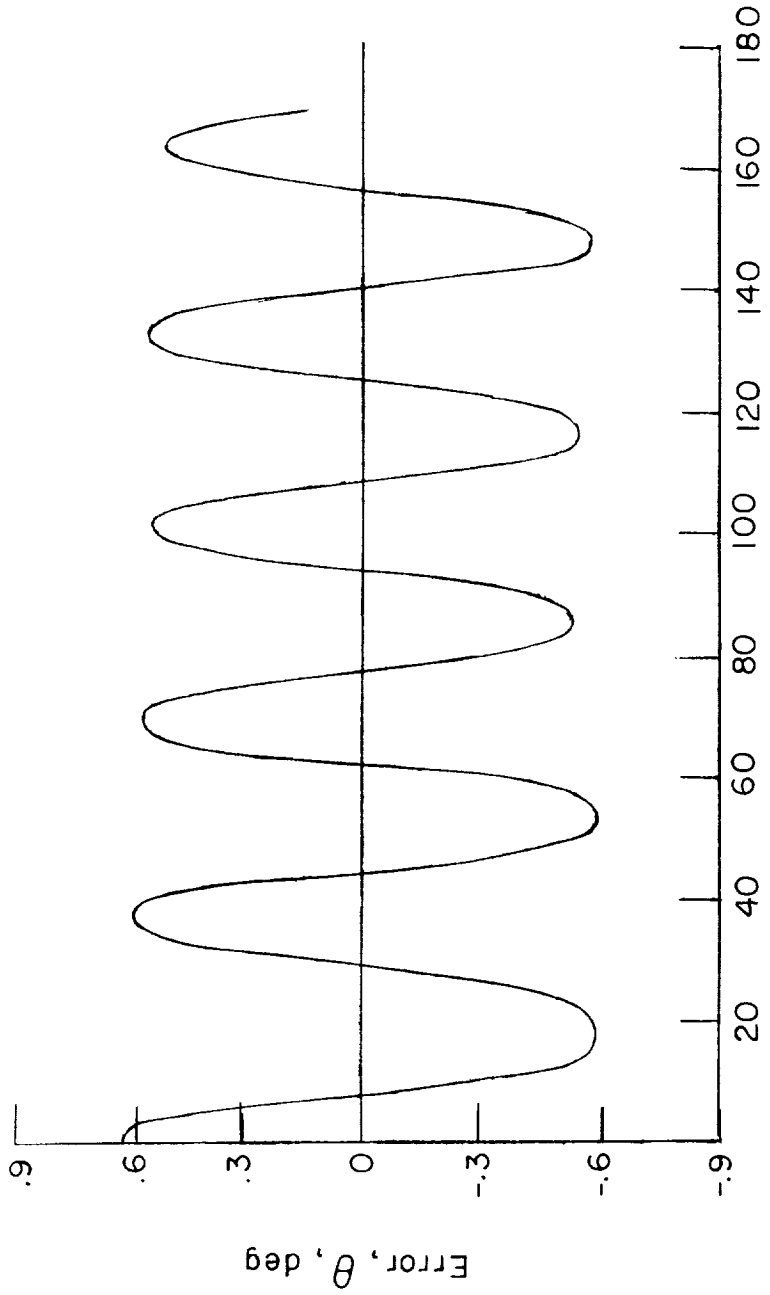

Figure 12.- Platform oscillation with no control damping.

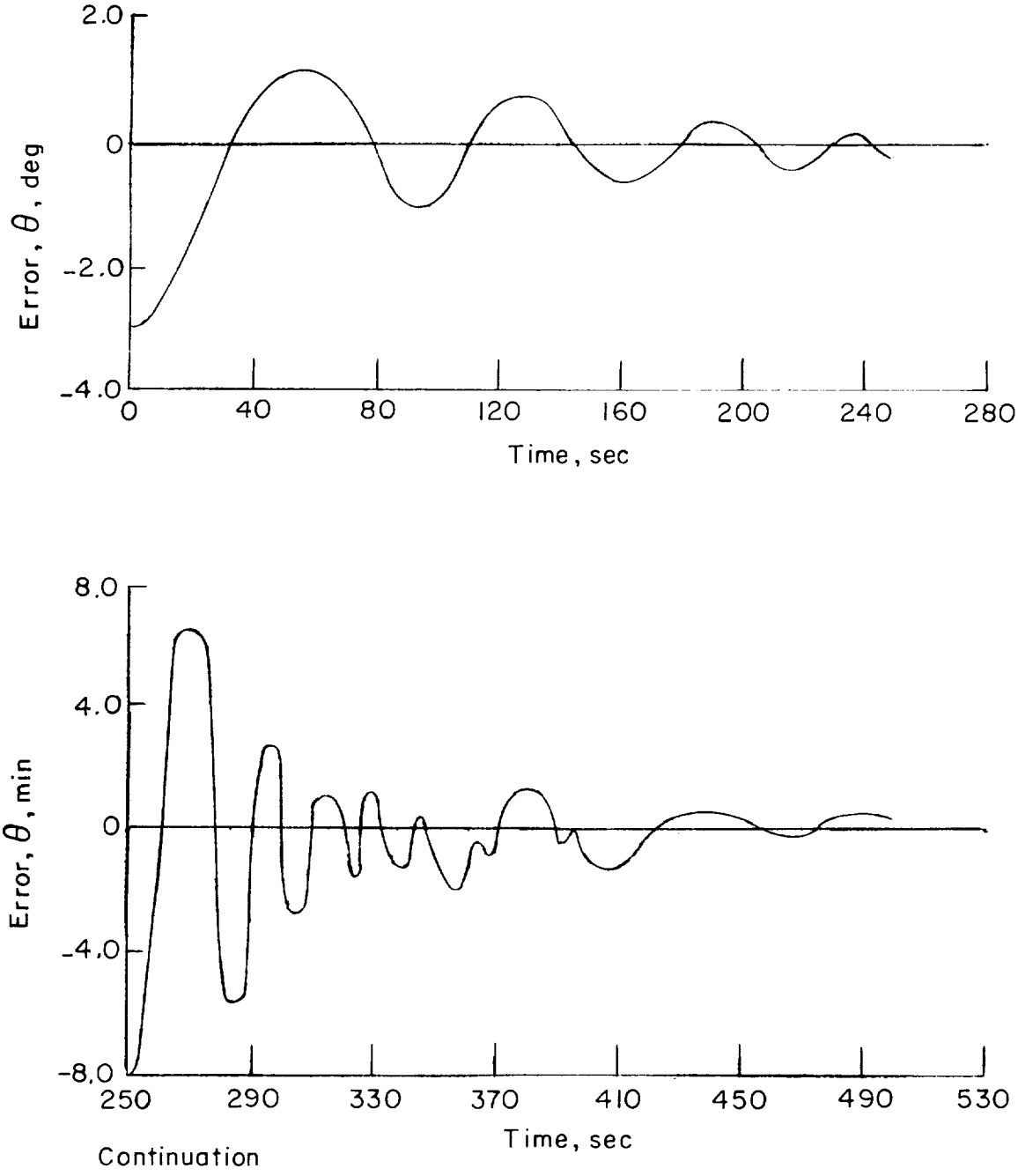

Figure 13.- Platform oscillation with capacitor lead. Note scale change of ordinate from degrees to minutes in lower plot.

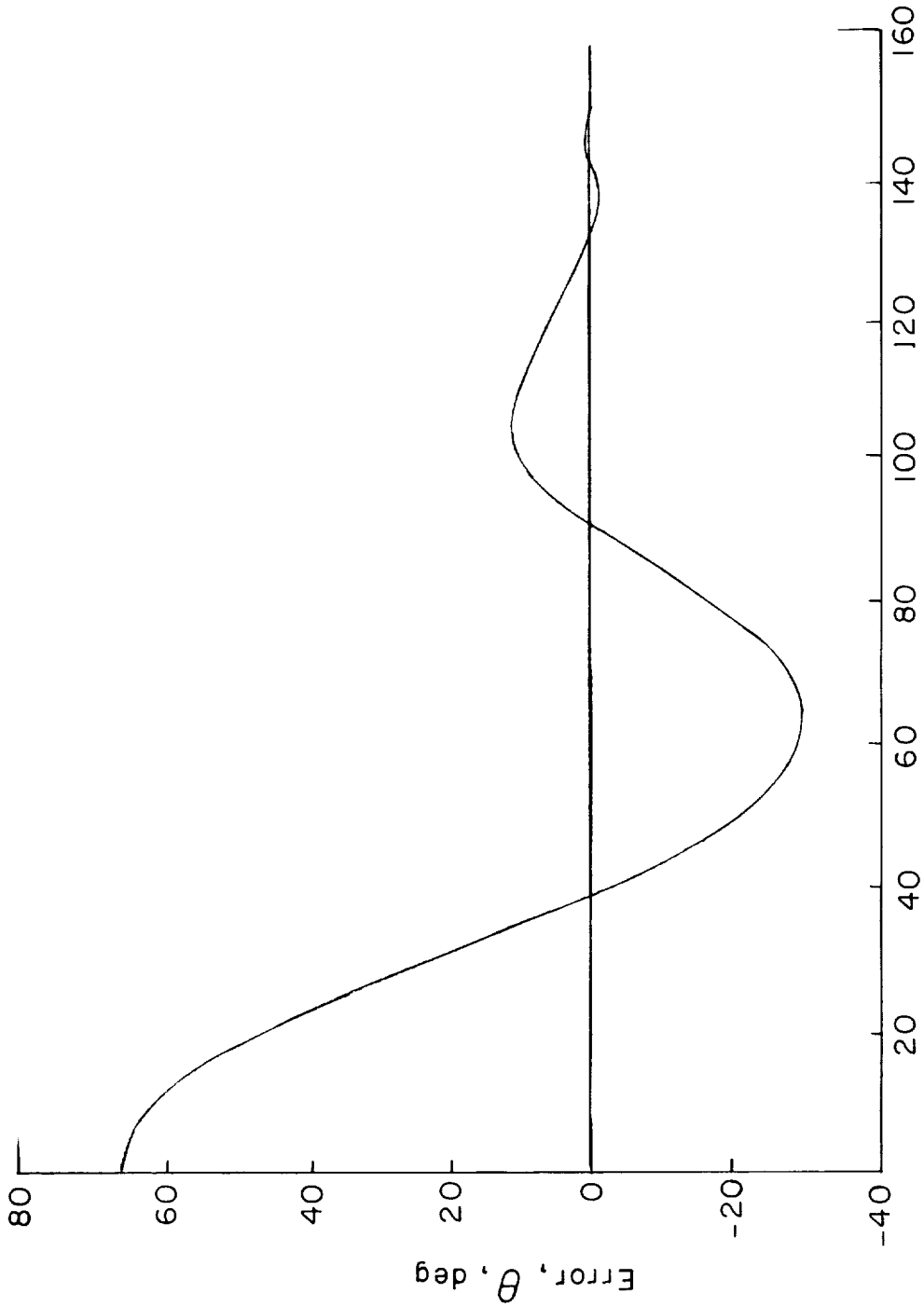

(a) Time history.

Figure 14.- Experimental system performance with rate limiting.

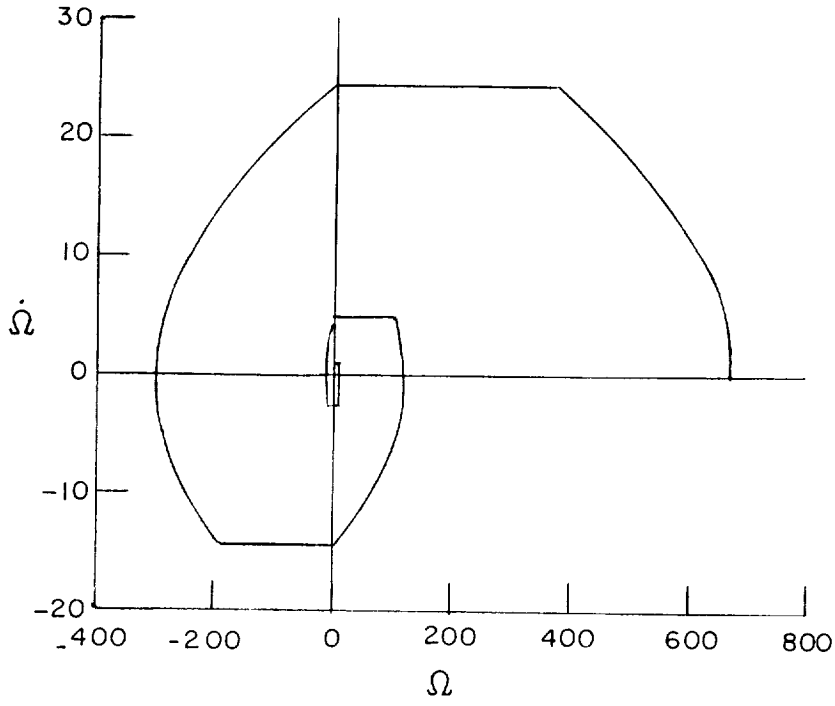

(b) Nondimensional phase plane plot. Large angle.

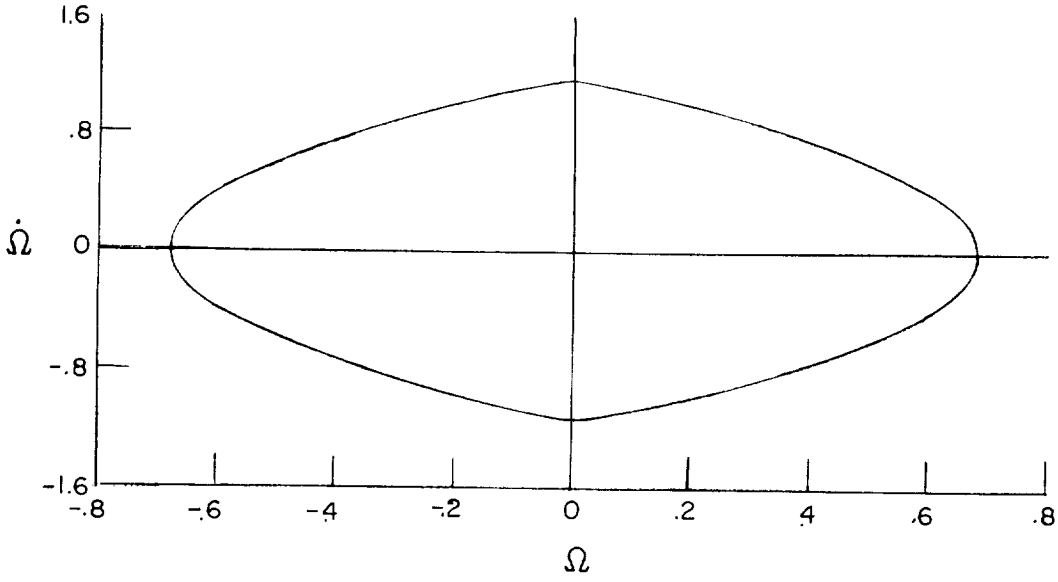

(c) Nondimensional phase plane plot. Small angle.

Figure 14.- Concluded.

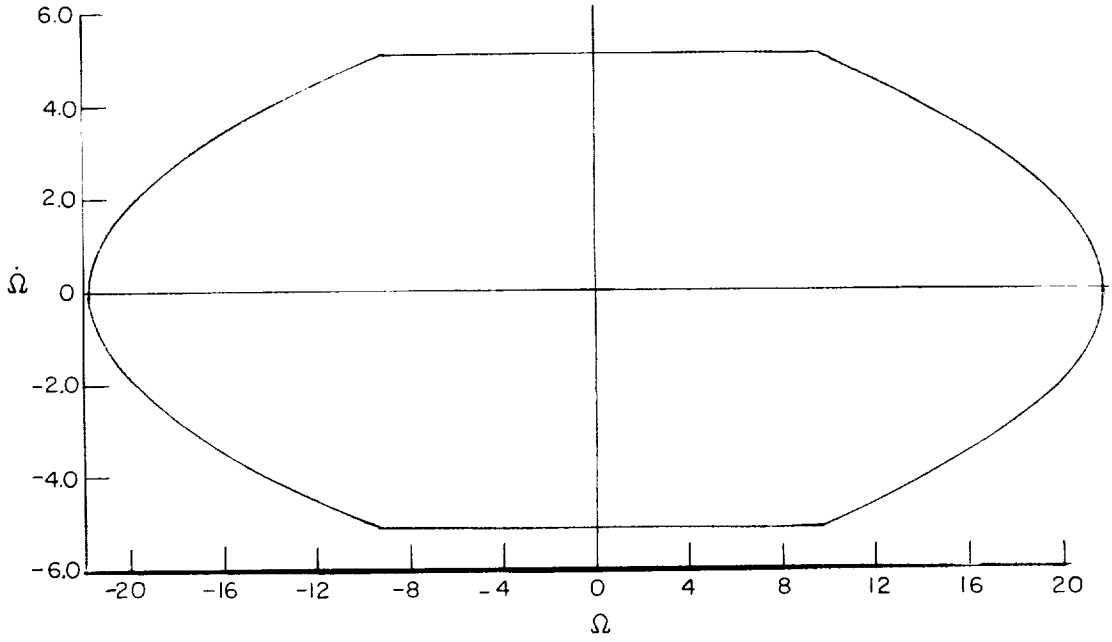

(a) Rate gain, 1.0; period, 27.5 seconds, valve-on time, 20.1 seconds.

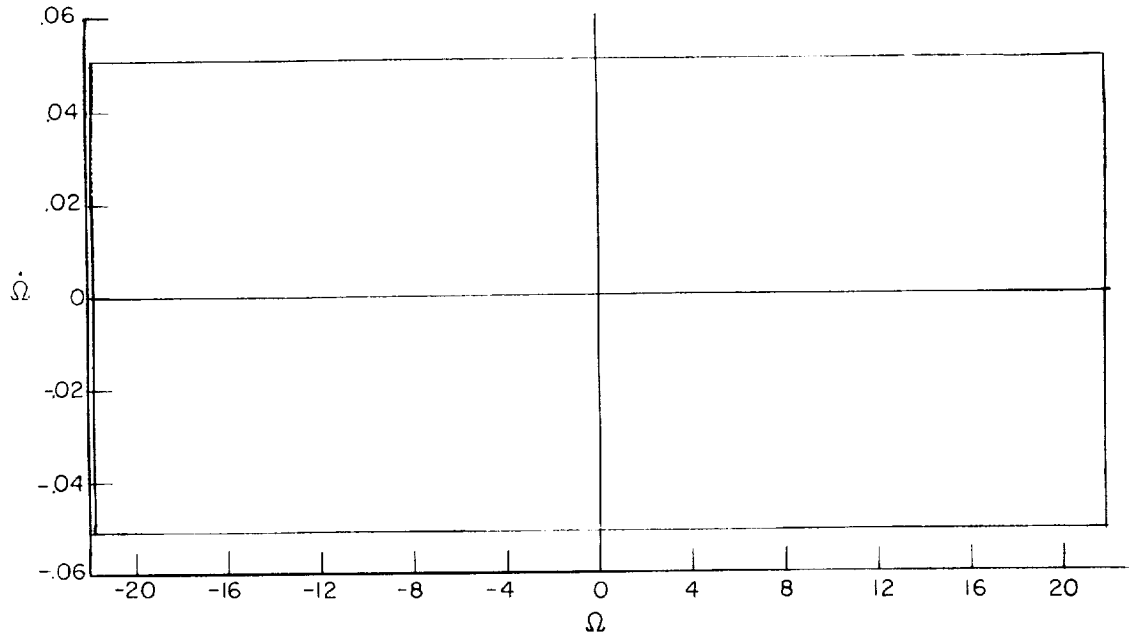

(b) Rate gain, 100; period, 0.483 hour; valve-on time, 0.2 second.

Figure 15.- Solar-power limit-cycle phase plane.

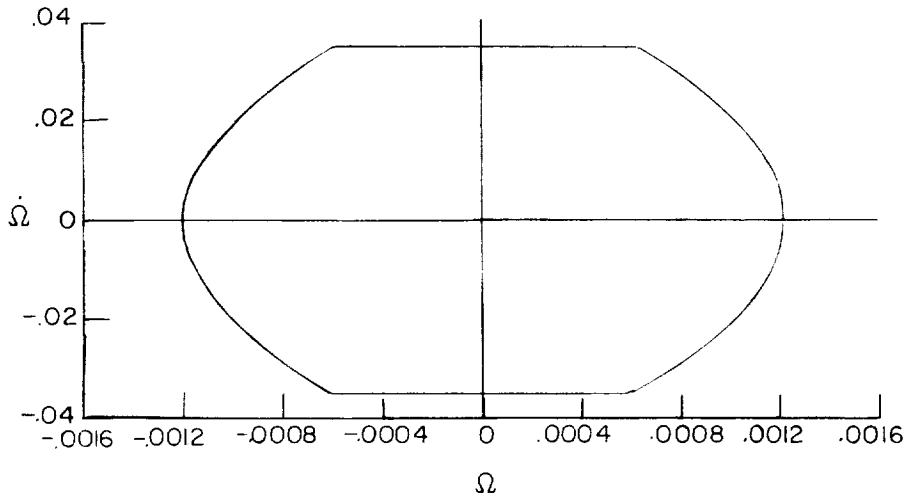

(a) Attitude gain, 10.0; rate gain, 143; period, 0.209 second; valve-on time, 0.14 second; total error, 0.2 second.

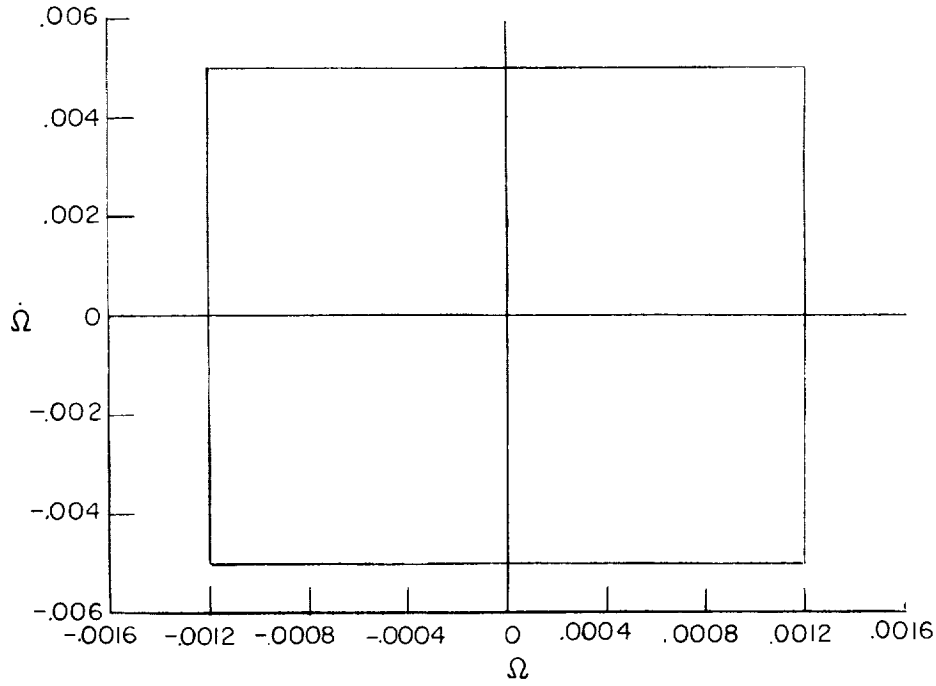

(b) Attitude gain, 5; rate gain, 1,000; period, 0.95 second; valve-on time, 0.02 second.

Figure 16.- Astronomical reference limit-cycle phase plane; I, 100 slug-feet^2; T, 0.04 foot-pound; total error, 0.2 second.

NASA-Langley, 1962 L-1944